Journal of Physics: Conference Series

PAPER • **OPEN ACCESS**

Imaging black holes with sparse modeling

To cite this article: Mareki Honma *et al* 2016 *J. Phys.: Conf. Ser.* **699** 012006

View the article online for updates and enhancements.

Recent citations

- Construction of Hamiltonians by supervised learning of energy and entanglement spectra
Hiroyuki Fujita *et al*

IOP ebooks™

Bringing you innovative digital publishing with leading voices to create your essential collection of books in STEM research.

Start exploring the collection - download the first chapter of every title for free.

This content was downloaded from IP address 46.105.103.191 on 01/05/2019 at 20:55

Imaging black holes with sparse modeling

Mareki Honma[1,2], Kazunori Akiyama[1,3,4], Fumie Tazaki[1], Kazuki Kuramochi[1,3], Shiro Ikeda[5,6], Kazuhiro Hada[1] and Makoto Uemura[7]

[1]Mizusawa VLBI Observatory, National Astronomical Observatory of Japan, Hoshigaoka, Ohshu, Iwate 023-0861, Japan
[2]Department of Astronomical Science, SOKENDAI (The Graduate University for Advanced Studies), Hoshigaoka, Ohshu, Iwate 023-0861, Japan
[3]Department of Astronomy, Graduate School of Science, The University of Tokyo, Hongo, Bunkyo-ku, Tokyo 113-0033, Japan
[4]Haystack Observatory, Massachusetts Institute of Technology, Route 40, Westford, MA 01886, USA
[5]Institute of Statistical Mathematics, Tachikawa, Tokyo 190-8562, Japan
[6]Department of Statistical Science, SOKENDAI (The Graduate University for Advanced Studies), Tachikawa, Tokyo 190-8562, Japan
[7]Astrophysical Science Center, Hiroshima University, Higashi-Hiroshima, Hiroshima 739-8526, Japan

E-mail: `mareki.honma@nao.ac.jp`

Abstract. We introduce a new imaging method for radio interferometry based on sparse-modeling. The direct observables in radio interferometry are visibilities, which are Fourier transformation of an astronomical image on the sky-plane, and incomplete sampling of visibilities in the spatial frequency domain results in an under-determined problem, which has been usually solved with 0 filling to un-sampled grids. In this paper we propose to directly solve this under-determined problem using sparse modeling without 0 filling, which realizes super resolution, i.e., resolution higher than the standard refraction limit. We show simulation results of sparse modeling for the Event Horizon Telescope (EHT) observations of super-massive black holes and demonstrate that our approach has significant merit in observations of black hole shadows expected to be realized in near future. We also present some results with the method applied to real data, and also discuss more advanced techniques for practical observations such as imaging with closure phase as well as treating the effect of interstellar scattering effect.

1. Introduction

Now it is believed that nearly all the galaxies harbor a super-massive black hole at their centers, and it is considered as the central engine of active galactic nuclei (AGN), which emit enormous amount of radiation from a compact region. Exactly speaking, however, the observational evidence obtained so far only reveals the existence of extremely dense objects, and there has been no direct confirmation that these compact and dense objects are real black holes surrounded by an event horizon, which is the critical radius within which even light cannot escape.

In order to obtain the direct confirmation of existence of black holes, one has to resolve the structure around a black hole at a scale of Schwarzschild radius. Detection of the black hole shadow, which is produced by unstable orbits of photons near the black hole, is the most

Content from this work may be used under the terms of the Creative Commons Attribution 3.0 licence. Any further distribution of this work must maintain attribution to the author(s) and the title of the work, journal citation and DOI.
Published under licence by IOP Publishing Ltd

direct confirmation of existence of black holes. Since the black holes are extremely compact, detection of the black hole shadows requires unprecedentedly-high angular resolution. As far as observations with electro-magnetic wave are concerned, the angular resolution of any telescope is roughly given by the ratio of the wavelength to the diameter of the telescope, namely,

$$\theta \approx \lambda/D. \tag{1}$$

Here θ is the angular resolution, λ is the wavelength, and D is the diameter of the telescope (or in case of radio interferometer, the maximum baseline). Currently, the highest angular resolution is given by VLBI (Very Long Baseline Interferometry, [1]), which utilizes the maximum baseline length corresponding to the diameter of the Earth (or even beyond by using an on-board radio telescope orbiting the Earth, e.g, VSOP launched by Japan or Russian Radio Astron satellite).

The largest black hole known so far (in terms of angular size) is Sgr A*, the supper-massive black hole at the center of our own Galaxy (the Milky Way). According to the most recent observations of stellar orbits around Sgr A*, the mass of Sgr A* is determined to be $4\times10^6 M_\odot$, where $M_\odot$ denotes the mass of the Sun. At a distance of 8 kpc, the angular size of Schwarzschild radius of Sgr A* is $\sim$10 μas (note that 1 μas corresponds to 10^{-6} arcsecond). The second largest black hole is the one at the center of a giant elliptical galaxy M87 located in the Virgo cluster. With an expected mass of 6×10^9 $M_\odot$ and an expected distance of 17 Mpc, the angular radius of M87's black hole is about 7 μas. Therefore, for resolving super-massive black holes, one requires an angular resolution at 10 μas level or higher. In order to achieve that high angular resolution, the EHT (Event Horizon Telescope) collaboration has been building a global VLBI array operating at a wavelength of 1.3 mm or shorter [2]. Pioneering observations of the EHT (with only three stations) have already detected compact structures in Sgr A* and M87 black holes corresponding to a scale of 4$\sim$5 Schwarzschild radii, demonstrating that mm-VLBI is in fact capable of resolving the structure in the vicinity of super-massive black holes [3, 4, 5].

Currently the EHT collaboration has extended the array to include more stations in US, Europe, Mexico, Chile, the Antarctica, and Green-land. Amongst these stations, the key is ALMA (Atacama Large Millimeter and sub-millimeter Array) located in Chile, because it has extremely-high sensitivity. In order to realize VLBI observations with ALMA, the international collaboration called APP (ALMA Phase-up Project) has recently completed the ALMA's VLBI capability. In fact, VLBI with ALMA will be plausibly in operation from ALMA Cycle-4, starting in early 2017.

However, even when the EHT with ALMA becomes available, one would require higher angular resolution than the array could provide at the initial phase. For instance, the initial observations of the full EHT is planned to be conducted at a wavelength of 1.3 mm, and when combined with the maximum baseline length of $\sim$9000 km, this provides an angular resolution of $\sim$25 μas. Meanwhile, the angular size of the black hole shadow is expected to be a few times of the Schwarzschild radius, and thus the angular resolution provided by the initial EHT may not be high enough to clearly resolve a black hole shadow. Another uncertainty is the mass of the black hole, with which the angular size of a black hole is linearly scaled. For instance, the black hole mass of M87 is still under debate and there exists a factor of two difference among the recent determinations of the black hole mass. This indicates that the angular size of the M87 black hole is also uncertain by a factor of two, and thus in case of smaller mass ($3 \times 10^9 M_\odot$, [6]), it may not be easy to resolve the black hole shadow even with the angular resolution of EHT.

In order to overcome this issue, we have been developing a new method of radio interferometric imaging based on sparse modeling (Honma et al. 2014, [7]), which significantly boost the angular resolution of image compared to the standard method currently used. In this paper we would like to introduce its basic concept as well as recent results of simulation and its application to real observational data.

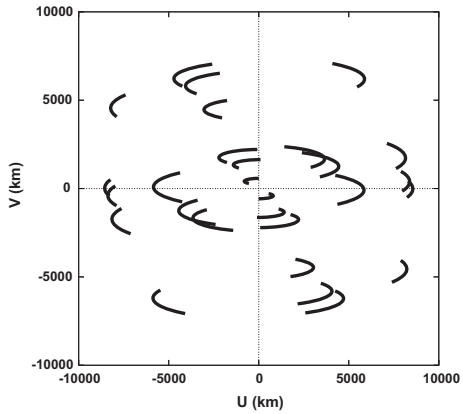

Figure 1. Simulated U-V coverage of the observations of M87 black hole with the six-station EHT array. Here U and V are shown in unit of km.

2. Radio Interferometry Imaging and Sparse Modeling

The basic equation between the direct observables (visibilities $\mathcal{V}$) and the image I is the two-dimensional Fourier transform [1], namely,

$$I(x, y) = \iint \mathcal{V}(u, v)\, e^{-2\pi i(ux+vy)}\, du\, dv. \tag{2}$$

Here the visibility $\mathcal{V}(u, v)$ is a function of spatial frequency (u, v), which is projected baseline length of interferometer normalized with the wavelength, i.e., $u \equiv U/\lambda$ and $v \equiv V/\lambda$, where U and V are physical lengths of the projected baselines. In theory, the parameters u and v should run from $-\infty$ to $+\infty$, but in practice this is impossible as the maximum U and V are limited by the longest baseline length. Practically, the Fourier transform in the above equation is executed as a discrete Fourier transformation over a finite range of sampling grids. Since the Fourier transformation is one-to-one conversion from visibility domain to image domain (and vice versa), to obtain an image with N^2 grids, one has to have full visibilities for N^2 grids in the u-v plane. However, sparse locations of VLBI stations make the sampling of the u-v space far from complete (e.g., see figure 1), and a large number of visibility grids in the u-v space remain un-sampled.

In the standard process of interferometric imaging, these un-sampled grids are filled with 0, which we call "0-filling". By doing this, one can conduct the Fourier transform from the visibility domain to the image domain. However, insertion of 0 to un-sampled grids causes severe degradation of the resultant image. In fact, it is this 0-filling process that causes infinite number of side lobes and finite beam size in the synthesized beam. Practically, the degradation of the images is corrected for by a method called CLEAN.

Sparse modeling provides a new approach to overcome above issues by directly solving the under-determined problem. This approach avoids 0-filling and thus consequently provides breakthrough for obtaining better resolution than the standard imaging with CLEAN algorithm.

As an introduction of sparse modeling, here we introduce lp-norm $||\mathbf{x}||_p$ as follows,

$$||\mathbf{x}||_p = ||\mathbf{x}||_0 \ \text{ for } p = 0, \tag{3}$$

$$||\mathbf{x}||_p = (\sum |x_i|^p)^{1/p} \ \text{ for } p > 0. \tag{4}$$

Here $||\mathbf{x}||_0$ describes the number of non-0 components of $\mathbf{x}$. Thus $l0$-norm directly represents the sparseness of the vector $\mathbf{x}$, i.e., if $l0$-norm is smaller, the vector $\mathbf{x}$ has more 0 components

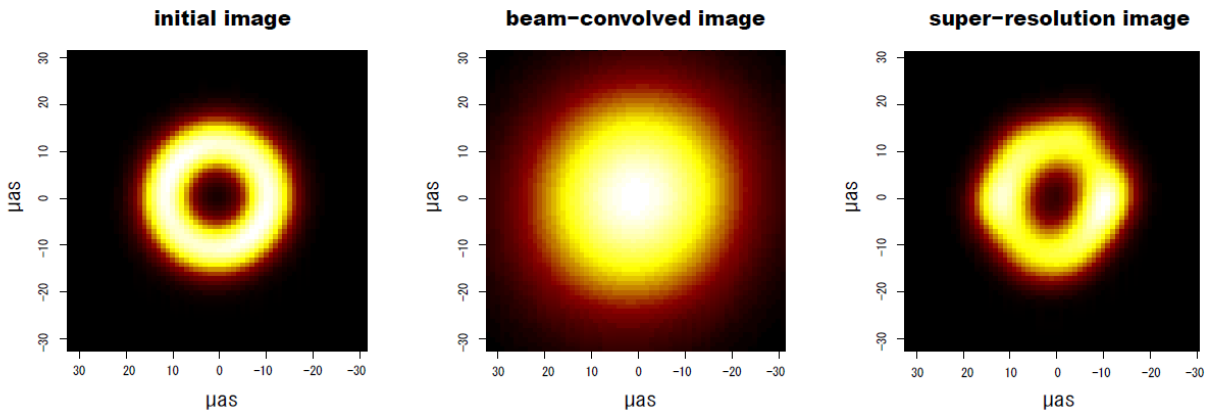

Figure 2. Simulated images of M87. From left to right, the initial model, the image with 0-filling, and the image with LASSO. Improvement of resolution in the LASSO image is significant.

and thus more "sparse". The basic idea of sparse modeling is to solve the under-determined problem by using the sparseness of the solution as regularizer, i.e., by selecting the optimal solution having the smallest $l0$-norm such as,

$$\mathbf{x} = \arg\min ||\mathbf{x}||_0 \text{ subject to } \mathbf{z} = \mathbf{A}\mathbf{x}. \tag{5}$$

Note that $\mathbf{z}$ is the observational quantities (visibilities in the present paper), $\mathbf{x}$ is the solution to be obtained (values of image grids), and $\mathbf{A}$ is the observational matrix (two-dimensional Fourier transform).

Practically speaking, finding the optimal solution with the smallest $l0$-norm requires huge computation cost because one has to try all the possible combinations of 0 components in $\mathbf{x}$. Therefore, obtaining an interferometry image using $l0$ is practically impossible. Instead, in this paper we alternatively use LASSO (Least Absolute Shrinkage and Selection Operator), which was originally developed by Tibshirani (1996) [8]. LASSO uses $l1$-norm to find the optimal solution from infinite number of solutions by,

$$\mathbf{x} = \arg\min \left(||\mathbf{z} - \mathbf{A}\mathbf{x}||_2^2 + \Lambda||\mathbf{x}||_1\right). \tag{6}$$

Here the first term in the argument describes goodness of fit, while the second term represents the penalty term based on the $l1$-norm. We note that Λ is a regularization parameter, which can be used to adjust the degree of sparsity by changing the weight of the $l1$-norm penalty.

Since the Fourier transformation given in equation (2) can be also written in a form of matrix (i.e., simultaneous linear equations), one can use LASSO to solve the under-determined equation in interferometer imaging.

3. Simulation

In order to demonstrate the capability of sparse modeling in interferometry imaging, here we first show the results of simulated observations of the super-massive black hole of M87 with the EHT. Here we consider the EHT array with six stations including CARMA (Combined Array for Research in Millimeter-wave, California, USA), SMTO (Submillimeter Telescope Observatory, Arizona, USA), JCMT (James Clerk Maxwell Telescope, Hawaii, USA), ALMA (Atacama Large Millimeter/submillimeter Array, Chile), LMT (Large Millimeter Telescope, Mexico), and IRAM (Institute de Radio Astronomie Millimétrique, Spain). All these stations are ready or nearly

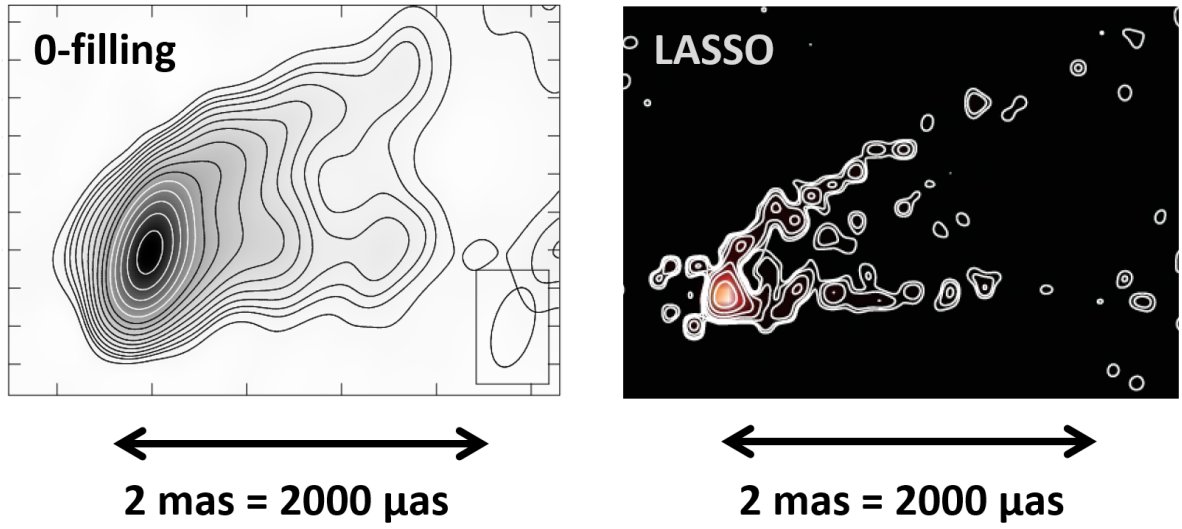

Figure 3. Standard and LASSO images of M87 observed with VLBA at a wavelength of 7 mm. In the two plots, exactly the same data are used. The angular resolution is better in the LASSO image, and the detailed structure of the M87 jet can be traced in more detail.

ready for VLBI observations at 1.3 mm, and the real data will become available within a few years from now on.

For the target source M87, we consider the smaller mass case with a black hole mass of $3 \times 10^9 M_\odot$ [6], for which resolving the black hole shadow would be more difficult. This corresponds to an angular size of the Schwarzschild radius of 4 μas at a source distance of 17 Mpc. The angular size of the black hole shadow is expected to be $\sim 20\ \mu as$, which is comparable or slightly less than the angular resolution (given by λ/D) of the EHT array operating at 1.3 mm. Figure 1 shows the u-v coverage of the simulated EHT array. As seen in the figure, the array provides relatively good sampling of the u-v plane, with maximum baselines of 8000 $\sim$ 9000 km in both north-south and east-west directions. However, it is obvious that there exist many "holes" in the u-v plane, where no visibility data are sampled. This under-sampling of the u-v plane makes the Fourier transformation in the interferometric imaging an under-determined problem.

In figure 2, we show the simulation results of M87 black hole images with the EHT. Here we assumed a simple doughnut-shape black hole shadow (the left panel), and created the simulated visibilities using the u-v coverage shown in figure 1 with a noise corresponding to $\sim$5% of the peak amplitude. Then we obtained the images of M87 by the standard method with 0-filling to un-sampled grids (the panel in the middle) and by LASSO (in the right). As shown in figure 2, imaging with LASSO provides better angular resolution and one can clearly trace the doughnut-shaped structure. Meanwhile, the standard imaging with 0-filling smears out the structure of the black hole shadow. This clearly demonstrates the merit of LASSO, which directly solves the under-determined problem of interferometric imaging.

4. Application to real data

We have seen that LASSO can provide a better angular resolution in interferometric imaging based on simulated data for the EHT observations. Here, to test if this applies to the real observations, we process the data of real VLBI observations in the same manner described above. For this purpose, here we use VLBA observations of M87 at 43 GHz obtained by Hada

et al.(2011) [9]. The observations were conducted toward the same target for the simulated EHT observations described above, but with a different array (10 stations of VLBA) and a different observing wavelength (7 mm). The resolution of the VLBA observations is not high enough to resolve a structure at a scale of the black hole shadow, but instead, the VLBA observations at 7 mm are powerful to trace the relativistic jet launched from the central black hole of M87 (e.g., [9]).

In figure 3, we show the resultant image of M87 obtained by the standard imaging (with 0-filling, left panel) and that by LASSO (right panel). Here the two images are reproduced from exactly the same data. Nevertheless, the LASSO image shows a dramatic improvement of the angular resolution, and it provides detailed structure of M87 jet: two most distinct features are a) clear separation of limb structures and b) obvious detection of the counter-jet components (to the left of the bright radio core in figure 3). The results presented here for the real VLBA observations clearly demonstrate the potential of sparse modeling technique for improving the angular resolution of the images. Hence, interferometric imaging with LASSO is expected to provide significant merit in studying the structure around the black hole and jet.

5. More advanced techniques

5.1. Imaging with closure phase

In the previous section, we implicitly assumed that we could obtain the full visibility information, i.e., both the amplitudes and phases of the complex visibilities. However, in practice, it is sometimes difficult to obtain the full visibilities because accurate calibration of phase is still an issue for mm VLBI. In fact, in the pioneering works of 1.3-mm observations of Sgr A* and M87 ([3, 4]), the only observables were amplitudes, and the phase information was totally missed and thus images are not yet available.

Recently there have been attempts to obtain the phases in mm VLBI, but obtaining complete phases (i.e., baseline-based visibility phase) is still difficult. Currently the only available information related with the phase is the closure phase, which is the phase term of the bi-spectrum defined as

$$\mathcal{V}_{123} = |\mathcal{V}_{12}||\mathcal{V}_{23}||\mathcal{V}_{31}|e^{i(\phi_{12}+\phi_{23}+\phi_{31})}. \tag{7}$$

Note that the closure phase $\phi_{123} \equiv \phi_{12} + \phi_{23} + \phi_{31}$ is obtained along a set of triangular baselines. The merit of introduction of the closure phase is that it is significantly easier to obtain compared to the individual baseline-based phase such as ϕ_{12}, ϕ_{23}, and ϕ_{31}. This is due to the fact that the largest error source of phase calibration is the tropospheric fluctuation at each station, and such station-based errors are totally canceled out when the closure is taken along the triangular baselines. In fact, recently Akiyama et al.[10] reports the first detection of closure phase in the VLBI observations of M87 at 1.3 mm. At the early phase of mm VLBI observations with ALMA, it is also expected that the available phase information could be limited to closure phases. The trade-off of closure phase is that one cannot describe the observational equation in a form of simultaneous linear equations, and the equation becomes non-linear. Therefore, it requires an iterative approach to handle the imaging with closure phase, and below we briefly discuss two possible approaches for this issue.

One way to deal with closure phase is to estimate the baseline-based phases from closure phases. Since the number of independent closure phases is always smaller than the number of independent baseline-based phases, this problem always becomes an under-determined problem, and this can be solved by techniques similar to sparse modeling, i.e., by introducing a reasonable regularizer. How to select an optimum regularizer depends on the nature of images. Ikeda et al.(2016)[11] proposes a method called PRECL (Phase REtrieval from CLosure phase), which uses smoothness of phase in the u-v plane as a regularizer: the phases should be similar if two baseline vectors are similar to each other, while the phases can be largely different if two baseline vectors are totally different. By introducing such a regularizer, Ikeda et al.[11] demonstrated

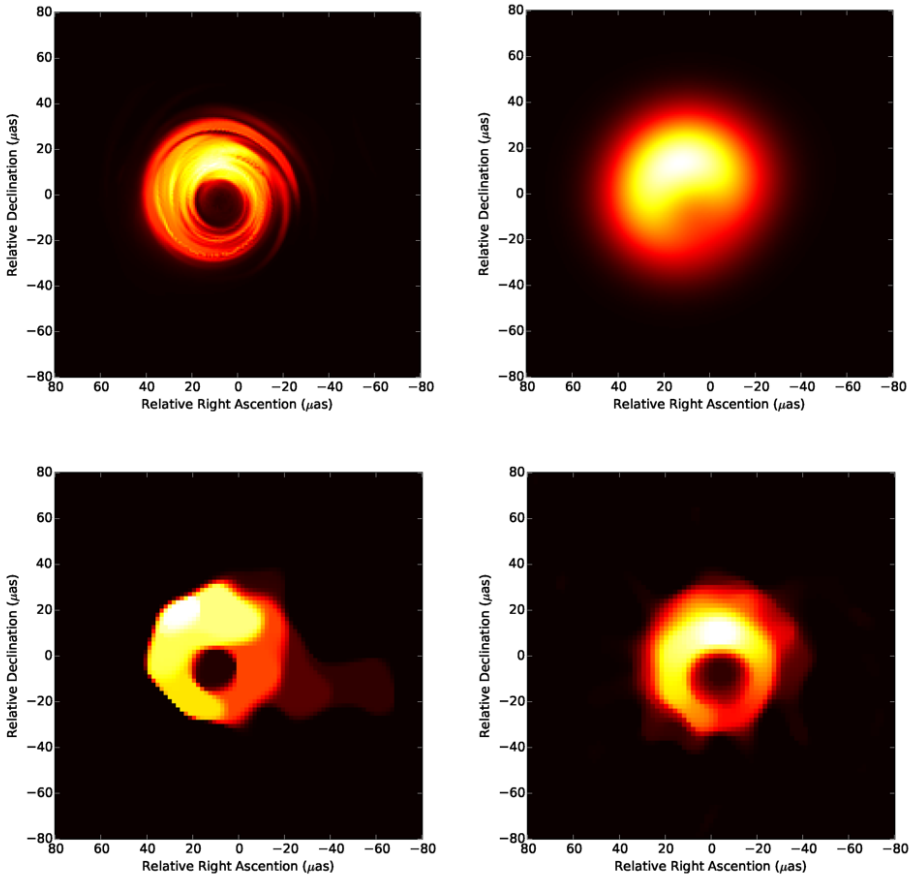

Figure 4. Imaging simulation of M87 using closure phase. The top left panel is the model by Dexter et al.[12], top right is the model convolved with a synthesized beam with 25 μas. The bottom left is the image with phase retrieval from closure (PRECL, [11]), and bottom right is the direct solution of non-linear problem based on iterative approach.

that the baseline-based phases can be well-reproduced from the closure phases using the real full-track interferometric observations with 10 stations. In figure 4, we show an example of more realistic model image of M87 black hole (Dexter et al. 2012, [12]) with the image constructed from closure phase using PRECL (bottom left of figure 4). Note that for the results in figure 4, in addition to the $l1$-norm we introduced another regularization term called the total variation (TV, see the next subsection) to obtain an effective angular resolution of the image. If this kind of method turns out to be applicable to general cases, this will introduce significant merit to the interferometric imaging, as this will simplify the phase calibration process of radio interferometer.

Another approach is to solve the non-linear problem directly by iteration. This can be done by calculating cost function (which includes model errors as well as sparsity term) and its gradient for a given image, and by searching for the image with the minimum cost based on iterative improvements of the image. Akiyama et al.[13] have shown that the practical algorithm such as L-BFGS-B [15, 16] can be used to solve such kind of problem at a practical computational cost. Of course, to obtain an optimum solution by an iterative process, the key is how to select the initial model in the iteration. Selecting a good initial model is still an open issue, but there are a few possible options to handle this problem. For instance, one may start with a low resolution image (small number of the grids) and use the result of low-resolution imaging as the initial

model for imaging with higher resolution. The bottom right panel of figure 4 shows the image obtained in such a way. Another possibility is to use other model to find an initial guess of images. The method like PRECL described above would be a good candidate for finding an initial image. The merit of the direct solution of the non-linear problem is that one can use regularizers in any form, such as non-linear cost function.

5.2. Optimal image resolution

A practical question on the super-resolution images obtained in the previous sections is: *what is the effective resolution of the images?* The effective resolution could be dependent of observational conditions such as the u-v coverage of the array and signal-to-noise ratio of the data. The most direct way to obtain the effective resolution is to use the data (and also the resultant images) themselves. As one of such approaches, here we propose to introduce the total variation (TV) term to the regularizer of the imaging equation, namely,

$$\mathbf{x} = \arg\min \left(||\mathbf{z} - \mathbf{A}\mathbf{x}||_2^2 + \Lambda ||\mathbf{x}||_1 + \Lambda_{\mathrm{TV}} \sum \sqrt{|I_{i+1,j} - I_{i,j}|^2 + |I_{i,j+1} - I_{i,j}|^2} \right), \tag{8}$$

where the subscripts i and j denote the indexes of image grids. The inclusion of the TV term will smoothen the image and by varying the weight of the TV term (Λ_{TV}), one can change the effective resolution of the image. Thus, by searching the optimum value of the parameter, one may determine effective resolution. Note that large Λ_{TV} results in resolution too low to reproduce the observed visibilities while too small Λ_{TV} would not introduce any improvement of goodness of fit in the visibilities. Thus, the optimum resolution may be determined by the image with Λ_{TV} that gives this transition in the goodness of fit.

5.3. Deblurring scattering effect

In the above discussion, we mainly focus on the case for M87. The other promising target for resolving the black hole shadow is Sgr A*, the super-massive black hole in our Galaxy. Since the angular size of Schwarzschild radius is expected to be $\sim$10 μas, the black hole shadow of Sgr A* should be larger than M87. Meanwhile, an issue for observing Sgr A* is the scattering effect due to the interstellar medium lying between the Earth and the Galactic center. In fact, the scattering effect is still non-negligible for VLBI observations at 1.3 mm. The main effect of the scattering can be described by a "Gaussian-kernel", which blurs the image of the black hole shadow. There have been studies to reconstruct a shadow image by deblurring the scattering effect (e.g., Fish et al. 2014, [14]). Since the main effect of the scattering is to worsen signal-to-noise ratio in particular at longer baselines, the effective resolution of the image will be degraded. To overcome this issue, we have been studying if sparse modeling approach is also effective for deblurring the scattered image of Sgr A*, which will be presented in a separate future work.

6. Future prospects

The new imaging techniques described above are all targeted at the forthcoming mm-VLBI observations (EHT) including ALMA (Atacama Large Millimeter/sub-millimeter Array). In order to make ALMA ready to conduct mm VLBI observations, the EHT collaboration and the ALMA Phase-up Project (APP) have brought VLBI capability to ALMA, and it is nearly completed. In fact, intercontinental VLBI fringes were successfully detected at both 4 mm and 1.3 mm with phase-up ALMA. Currently it is planned to open ALMA's VLBI capability for ALMA Cycle-4, which will be called in 2016 spring, and actual observations will be expected to start in early 2017. Therefore, we will obtain real mm-VLBI data in late 2017 or early 2018, and with the techniques described above hopefully we will be able to detect the black hole shadow for the first time.

Acknowledgments
The present study was financially supported by MEXT/JSPS grant-in-aid for innovative area (KAKENHI No 25120007).

References
[1] Thompson A R, Moran J M and Swenson G W Jr 2001 *Interferometry and Synthesis in Radio Astronomy*, 2nd edition (New York: Wiley-Interscience)
[2] Doeleman S S, Fish V L, Broderick A E, Loeb A and Rogers A E E 2009 *Astrophys. J.* **695** 59
[3] Doeleman S S et al. 2008 *Nature* **455** 78
[4] Doeleman S S et al. 2012 *Science* **338** 355
[5] Fish V et al. 2011 *Astrophys. J.* **726** 36
[6] Gebhardt K and Thomas J 2009 *Astrophys. J.* **700** 1690
[7] Honma M, Akiyama K, Uemura M and Ikeda S 2014 *Publ. Astron. Soc. Japan* **66** 95
[8] Tibshirani R 1996 *J. R. Statist. Soc.* B **58** 267
[9] Hada K et al. 2011 *Nature* **477** 185
[10] Akiyama K et al. 2015 *Astrophys. J.* **807** 150
[11] Ikeda S et al. 2016 submitted to *Publ. Astron. Soc. Japan*
[12] Dexter J, McKinney J C and Agol E 2012 *Mon. Not. R. Astron. Soc.* **421** 1517
[13] Akiyama K et al. 2016 in preparation
[14] Fish V et al. 2014 *Astrophys. J.* **795** 134
[15] Byrd R H, Lu P and Nocedal J 1995 *SIAM J. Sci. Stat. Com.* **16** 1190
[16] Zhu C, Byrd R H and Nocedal J 1997 *ACM Trans. Math. Soft.* **23** 550